# Neutron scattering from the static and dynamic lattice of $SrCu_2(BO_3)_2$ in its Shastry-Sutherland singlet ground state

S. Haravifard,[1,*] B. D. Gaulin,[1,2,3] Z. Yamani,[4] S. R. Dunsiger,[1,†] and H. A. Dabkowska[3]

[1]*Department of Physics and Astronomy, McMaster University, Hamilton, Ontario, Canada L8S 4M1*

[2]*Canadian Institute for Advanced Research, 180 Dundas Street West, Toronto, Ontario, Canada M5G 1Z8*

[3]*Brockhouse Institute for Material Research, McMaster University, Hamilton, Ontario, Canada L8S 4M1*

[4]*Canadian Neutron Beam Centre, NRC, Chalk River Laboratories, Chalk River, Ontario, Canada K0J 1J0*

(Received 22 December 2011; published 12 April 2012)

Elastic and inelastic neutron scattering results show that $SrCu_2(BO_3)_2$ enters its low-temperature singlet ground state below 10 K without an obvious accompanying structural phase transition, despite suggestions emanating from earlier heat capacity measurements. However, evidence for significant spin-phonon coupling is found in the energy widths, and the corresponding lifetimes, of transverse acoustic phonons propagating in the ($H$00) direction of the Shastry-Sutherland, tetragonal basal plane. Transverse acoustic phonons with energies comparable to and higher than the onset of the two-triplet continuum show substantially increased lifetimes on entering the singlet ground state below ∼10 K. This is qualitatively consistent with the removal of a decay channel for the phonons due to the gapping of the spin excitation spectrum in $SrCu_2(BO_3)_2$ at low temperatures.

DOI: 10.1103/PhysRevB.85.134104 PACS number(s): 63.20.kk, 75.40.Gb

## I. INTRODUCTION

The novelty of the ground states of quasi-two-dimensional quantum magnets displaying collective singlet or spin gap behavior and the relation of these materials to high-temperature superconductivity in the copper oxides have been cause for great interest.[1] There are, however, relatively few examples of such materials, and the difficulties in crystal growth have further added to the challenges for the study of these systems.

$SrCu_2(BO_3)_2$ is a realization of the two-dimensional Shastry-Sutherland model[2] for interacting $S = 1/2$ dimers.[3,4] It has been well studied and is known to possess a nonmagnetic ground state. $SrCu_2(BO_3)_2$ is comprised of well-separated layers of $Cu^{2+}$, $S = 1/2$ orthogonal dimers on a square lattice and it crystallizes into the tetragonal space group $I42m$ with lattice parameters $a = 8.995$ Å, $c = 6.649$ Å at room temperature.[5] Earlier neutron[6–9] and ESR spectroscopy[10,11] studies have established the leading terms in the $SrCu_2(BO_3)_2$ microscopic Hamiltonian as

$$\mathcal{H} = J \sum_{nn} \mathbf{S_i} \cdot \mathbf{S_j} + J' \sum_{nnn} \mathbf{S_i} \cdot \mathbf{S_j}, \qquad (1)$$

where $J$ and $J'$ are the exchange interactions within the dimers and between $S = 1/2$ spins on neighboring dimers, respectively. Both the exchange interactions $J$ and $J'$ are antiferromagnetic. It has been shown that subleading Dzyaloshinskii-Moriya (DM) interactions weakly split the three one-triplet modes excited out of the singlet ground states, even at zero applied magnetic field.[7–9,12]

Theoretically, a small enough value for the ratio of $x = \frac{J'}{J}$ would mean that such a quantum magnet possesses a singlet ground state.[13] The ratio $x$ has been estimated to be between 0.60 and 0.68 for $SrCu_2(BO_3)_2$. These estimates place it on the low side of the critical value of $x$ at which a quantum phase transition occurs between a collective singlet state and a four-sublattice Néel state at zero temperature.

At low temperatures and in a finite magnetic field, much interest has focused on a finite magnetization which develops at sufficiently high magnetic fields, wherein the lowest energy of the three-triplet states is driven to zero energy.[4,14–17] This is related to Bose-Einstein condensation of the triplet excitations, and in $SrCu_2(BO_3)_2$ occurs for fields near and above 20 T. On further raising the magnetic field, plateaus have been observed in the magnetization which have been interpreted in terms of preferred filling of the singlet ground state with increasing densities of triplet excitations.[16,17]

As described above, the study of this material has been mostly focused on the magnetic properties of this system. However, recently there has been increasing interest in the possible role of spin-lattice effects in $SrCu_2(BO_3)_2$. It has been suggested that there is an important relation between spin-lattice interactions in $SrCu_2(BO_3)_2$ and its magnetic dynamics at low temperatures and high magnetic fields.[3,18,19] Such a strong interplay between lattice and magnetic properties is a well-known and characteristic aspect of certain low-dimensional quantum spin systems, especially quasi-one-dimensional spin Peierls systems.[20–22] In $SrCu_2(BO_3)_2$ a lattice distortion has been suggested as a mechanism to stabilize the spin superstructure associated with the 1/8 magnetization plateau, for example, the first observation of such a magnetization plateau in a quasi-2D material.[15] More generally, lattice distortions in $SrCu_2(BO_3)_2$ have the potential to allow magnetic interactions which are otherwise forbidden in a more symmetric environment, as they lower the crystal symmetry.[7] For example, buckling of the $CuBO_3$ planes allows certain components of DM interactions to be nonzero. As previously mentioned, these subleading DM interactions weakly split the three triplet modes even in zero applied magnetic field.[7–9] Recent infrared spectroscopy measurements with polarized light on $SrCu_2(BO_3)_2$ have revealed a relatively high energy optic phonon excitation in the $a$-$b$ plane which splits below 15 K.[23] In addition, a recent powder neutron diffraction study of $SrCu_2(BO_3)_2$ has shown the temperature dependence of the tetragonal lattice parameters to mimic the temperature dependence of the uniform susceptibility at low temperatures, as the system enters its nonmagnetic singlet ground state.[24] These observations indicate that significant spin-lattice coupling is manifest within the singlet ground

 

state of $SrCu_2(BO_3)_2$. For these and related reasons a careful study of the crystalline structure and vibrational modes of $SrCu_2(BO_3)_2$ is of interest. In this paper we report a neutron diffraction confirmation that the tetragonal crystal structure of $SrCu_2(BO_3)_2$ is maintained down to 3.8 K in our samples. Most importantly we report a new study of the low-energy normal modes of vibration within this structure, the acoustic phonons, in a single crystal of $SrCu_2(BO_3)_2$ as the sample was cooled from the paramagnetic state into its singlet ground state below ∼10 K.

## II. EXPERIMENTAL DETAILS

The $SrCu_2(^{11}BO_3)_2$ single crystal studied was the same high-quality single crystal employed in previous magnetic neutron scattering experiments.[9] It was grown by floating zone image furnace techniques at a rate of 0.2 mm/hour in an $O_2$ atmosphere. The crystal was approximately cylindrical in shape, with approximate dimensions of 4.5 cm in length by 0.6 cm in diameter. The sample was grown using $^{11}B$, to avoid the high neutron absorption cross section of natural boron. Powder neutron diffraction measurements were performed on a fine powder sample of $SrCu_2(^{11}BO_3)_2$ using 2.37 Å and 1.3 Å neutrons at the C2 diffractometer of the Canadian Neutron Beam Centre (CNBC), Chalk River Laboratories. The powder sample was loaded in an Al sample cell (4.5 cm in length and 0.6 cm in diameter) in the presence of a He exchange gas and mounted in a pumped $^4He$ cryostat. These powder diffraction measurements were preformed as a function of temperature from 3 K to 20 K.

Inelastic neutron scattering measurements were performed on the single crystal of $SrCu_2(^{11}BO_3)_2$ using the C5 triple-axis spectrometer at CNBC, Chalk River. The crystal was mounted in a He cryostat with its $(H, K, 0)$ plane coincident with the horizontal plane, such that wave vectors near the $\mathbf{Q} = (4, 0, 0)$ zone center could be accessed. These measurements employed pyrolitic graphite (PG) as both monochromator and analyzer crystals, and used a fixed final neutron energy of 14.7 meV. A PG filter was placed in the scattered beam to eliminate higher order contamination.

## III. POWDER NEUTRON DIFFRACTION MEASUREMENTS

$SrCu_2(BO_3)_2$ displays a tetragonal crystal structure characterized by stackings of $CuBO_3$ and Sr planes along the $c$ direction.[5,18,19] Within the $CuBO_3$ layer, $BO_3$ molecules form a triangle and the $Cu^{2+}$ ions are connected through the $BO_3$ molecules. All the $Cu^{2+}$ ions are located at crystallographically equivalent sites and have a spin $S = 1/2$ magnetic moment associated with them. Each $Cu^{2+}$ ion has one nearest-neighbor $Cu^{2+}$ ion and four next-nearest-neighbor $Cu^{2+}$ ions in the plane. A pair of nearest-neighbor $Cu^{2+}$ ions are connected through O sites, which are vertices of the $BO_3$ triangles, and form a dimer unit. The dimer units are connected orthogonally through $BO_3$ molecules. The distance between the nearest-neighbor $Cu^{2+}$ ions is 2.905 Å, and that between the next-nearest-neighbor $Cu^{2+}$ ions is 5.132 Å at room temperature. Figure 1 shows a unit cell of $SrCu_2(BO_3)_2$ within the tetragonal $a$-$b$ plane, projected along the $c$ direction. Sparta *et al.*[19]

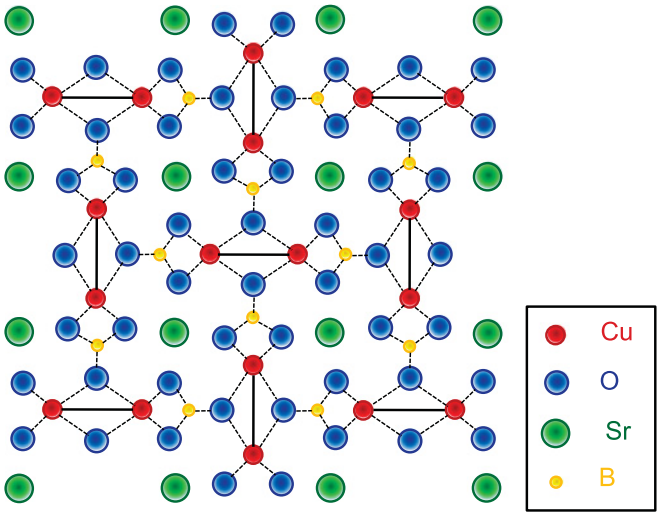


FIG. 1. (Color online) A schematic view of the basal $a$-$b$ plane structure of $SrCu_2(BO_3)_2$ is shown. The green, $Sr^{2-}$ ions lie in a plane displaced out-of-the-page relative to the buckled $Cu(BO_3)_2$ planes. The red ions joined by solid lines highlight the $Cu^{2+}$ dimers.

reported x-ray diffraction measurements showing a structural phase transition occurring in $SrCu_2(BO_3)_2$ at $T_s = 395$ K, taking it from the space group $I\,4\,2$ to $I\,4/m$ cm (both tetragonal).[19] Below $T_s$ there is a buckling in the $CuBO_3$ plane, while above $T_s$ the dimers within a unit cell lie in the same plane, making the $CuBO_3$ plane a mirror plane. The existence of a mirror plane is important for possible DM interactions. Above $T_s$, the DM interactions may exist only for the next-nearest-neighbor $Cu^{2+}$ pairs and do not exist for the nearest-neighbor pairs, since the middle of a nearest-neighbor bond possesses an inversion center. However, below $T_s$, the mirror plane is lost; therefore, DM interactions can exist for both next-nearest-neighbor pairs and nearest-neighbor pairs.

Jorge *et al.* performed specific-heat measurements on $SrCu_2(BO_3)_2$ in a continuous magnetic field $H$ up to 33 T.[16] They argued that an intradimer DM interaction, which violates the observed crystal symmetry at temperatures below $T_s = 395$ K, is required to explain the low-temperature specific heat of $SrCu_2(BO_3)_2$ in magnetic fields $H \sim 18$ T.[7,11] Jorge *et al.* proposed a possible structural phase transition at low temperatures that lowers the crystal symmetry allowing a nonzero value for the $z$ component of the nearest-neighbor DM interaction.[16] The crystal symmetry of the system affects the DM interactions and consequently may modify the thermal and magnetic properties of the material. The proper inclusion of such small, subleading terms in the spin Hamiltonian would allow, in principle, for an improved theoretical understanding of $SrCu_2(BO_3)_2$ and better accounting for the experimental results.

Vecchini *et al.*[24] carried out a thorough powder neutron diffraction study of $SrCu_2(BO_3)_2$ to low temperatures. This study showed that $SrCu_2(BO_3)_2$ displays subtle modifications to the structure that occur below ∼34 K, and interesting temperature dependencies in its structural parameters to low temperatures, but that it retains its tetragonal crystal structure to ∼2 K.

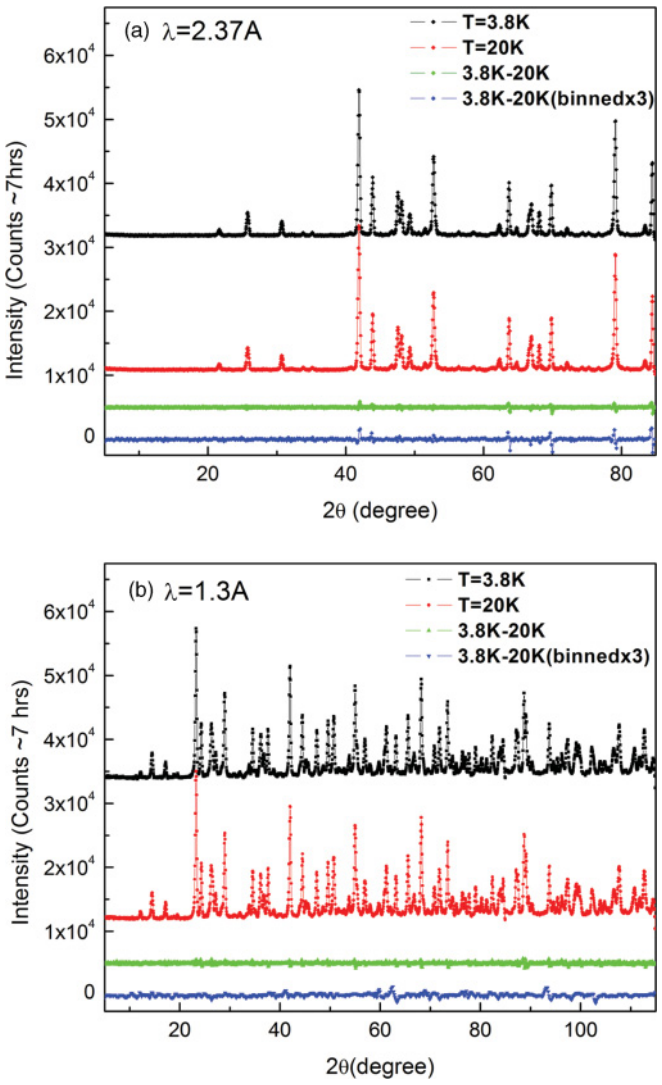


FIG. 2. (Color online) Powder neutron diffraction from $SrCu_2(BO_3)_2$ taken at $T = 3.8$ K and $T = 20$ K is shown using neutrons of wavelength $\lambda = 2.37$ Å (a) and $\lambda = 1.3$ Å (b). Also plotted in both panels are the subtracted data sets from the two temperatures which show no evidence for a structural distortion on cooling $SrCu_2(BO_3)_2$ into the singlet ground state below ~10 K.

As the Jorge *et al.*[16] specific-heat measurements were performed on samples from the same crystal growth laboratory at McMaster University, and using the same crystal growth protocols as employed in the growth of the materials reported in this paper, we felt it prudent to reexamine the low-temperature structure of the present $SrCu_2(BO_3)_2$ material. Figure 2 shows the results of the new neutron diffraction measurements performed on $SrCu_2(BO_3)_2$. Figure 2(a) shows the results for $\lambda = 1.3$ Å at 3.8 K and 20 K temperatures while Fig. 2(b) shows the results for $\lambda = 2.37$ Å at 3.8 K and 20 K temperatures. In both figures, black squares and red circles represent the data collected at 3.8 K and 20 K, respectively. The difference between the measurements at these two temperatures was calculated and the green upward triangles represent the subtracted values. The blue downward triangles show the subtracted values binned to help visualize any weak variation between the two data sets well within and well above the singlet ground state. No such temperature-dependent behavior is observed, implying that any possible structural phase transitions involves changes in Bragg intensity at the 1 part in $10^3$ level or lower. We therefore conclude that $SrCu_2(BO_3)_2$ retains its tetragonal structure down to the lowest temperatures measured, ~2 K, consistent with the earlier results reported by Vecchini *et al.*[24]

## IV. NEUTRON SCATTERING MEASUREMENTS OF ACOUSTIC PHONONS

Measurements of the spectrum of transverse and longitudinal acoustic phonons propagating in the $(H, 0, 0)$ direction of $SrCu_2(BO_3)_2$ were performed using triple-axis neutron spectrometry and the C5 spectrometer at the CNBC, Chalk River. Constant-**Q** measurements were performed along $(4, K, 0)$ to preferentially measure transverse acoustic phonons, and along $(4 + H, 0, 0)$ to preferentially measure longitudinal acoustic phonons. These measurements employed pyrolitic graphite (PG) as both vertically focused monochromator and analyzer. Measurements were performed in constant-$E_f$ mode using $E_f = 14.7$ meV and a PG filter was placed in the scattered beam to remove harmonic contamination.

Two sets of measurements were performed employing different collimation between the components of the instrument. Collimation of [none, 0.48°, 0.55°, 1.2°], using the convention [source-monochromator, monochromator-sample, sample-analyzer, analyzer-detector], resulting in an approximate energy resolution of ~1 meV, was employed to survey the low-lying phonons with energies below ~25 meV. These measurements, which are shown as a color contour map in Fig. 3, were performed at 150 K so as to thermally populate all of the acoustic phonons. Another set of relatively high resolution measurements were performed using tighter collimation [none, 0.273°, 0477°, 1.2°], and resulting in energy resolution of 0.5 meV. In all cases, the single-crystal sample was mounted in a closed-cycle refrigerator in the presence of a He exchange gas allowing us to access temperatures as low as 3 K with a temperature stability of ~0.05 K.

The survey of the longitudinal and transverse acoustic phonons propagating along $(H, 0, 0)$ displayed in Fig. 3 shows the transverse phonon branch to be consistently lower in energy than the longitudinal branch, as expected, with zone boundary energies on ~10 and 15 meV, respectively. Note that although the $\mathbf{Q} = (4, K, 0)$ scan in the top panel of Fig. 3 shows only the transverse acoustic phonon, as expected from the $(\epsilon \cdot \mathbf{Q})^2$ term in the phonon cross section, the $\mathbf{Q} = (4 + K, 0, 0)$ scan in the bottom panel of Fig. 3 shows both the longitudinal and transverse acoustic phonons. Presumably this is a consequence of finite out-of-scattering plane resolution which feeds some of the transverse acoustic polarization into a nominally clean measurement of the longitudinal acoustic phonons. Figure 3 also shows that the lowest optic phonon energy at the Brillouin zone center is ~17 meV, in agreement with optical studies of $SrCu_2(BO_3)_2$.[23]

We were particularly interested in potential phonon-magnon coupling associated with the formation of the singlet

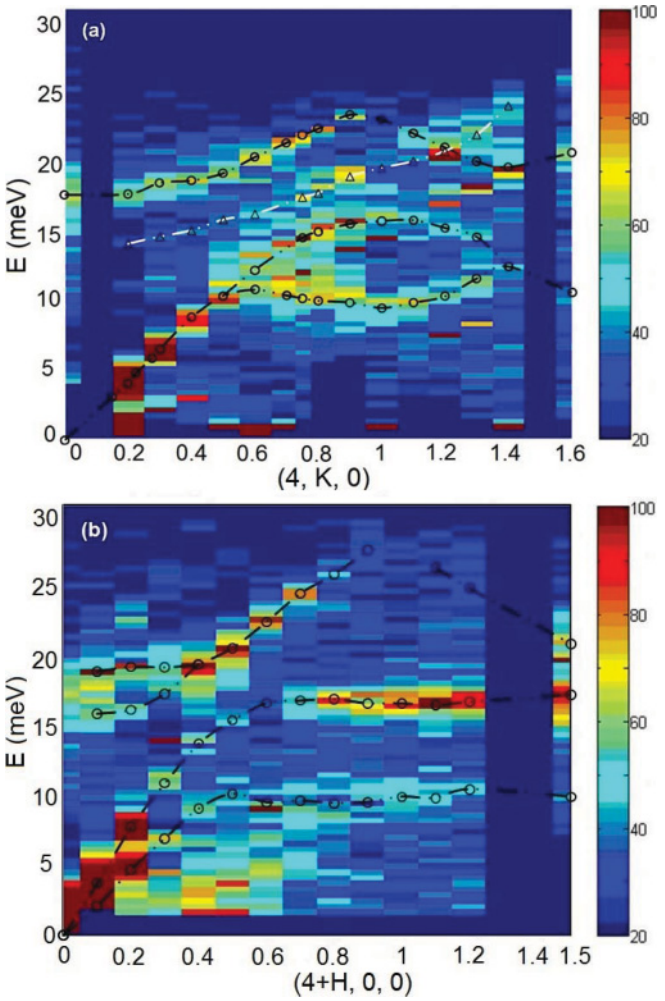


FIG. 3. (Color online) Color contour maps summarizing neutron scattering primarily from transverse acoustic (top) and longitudinal acoustic phonons in single-crystal $SrCu_2(BO_3)_2$. Constant-**Q** measurements at (4, $K$, 0) (top) and (4 + $H$, 0, 0) (bottom) measure primarily transverse and longitudinal phonon modes, respectively. All data were taken at $T = 150$ K. Typical (4, $K$, 0) constant-**Q** scans at lower temperatures are shown in the left-hand panels of Fig. 4.

spin state in $SrCu_2(BO_3)_2$ below ∼10 K. The gapping of the magnetic spectrum at low energies and formation of one- and two-triplet excitation bands at low temperature has the potential to couple strongly to the low-lying phonons, as the gapped magnetic excitation spectrum may eliminate a decay channel for low-lying phonons. This would result in longer phonon lifetimes within the singlet ground state. The relevant constant-**Q** measurements were performed with tighter collimation and higher energy resolution of 0.5 meV as the anticipated effects on phonon lifetimes were relatively small, and thus higher energy resolution was desirable. Although measurements were performed on both longitudinal and transverse acoustic phonons, focusing effects, and the fact that the energy resolution is better at lower energies, led to better resolution and intensity associated with the low-energy transverse acoustic phonons. We will therefore restrict our discussion to constant-**Q** measurements of the form (4, $K$, 0) which probe the transverse acoustic phonons.

Our (4, $K$, 0) constant-**Q** measurements were performed at temperatures of 3, 9, 15, 30, and 100 K, spanning a range from well below to well above the onset of the singlet ground state as identified by the rollover in the low-temperature susceptibility near 10 K, signifying entrance into the nonmagnetic ground state. We chose to study **Q**'s of the form (4, $K$, 0) with $K$ ranging from 0.1 to 0.275, such that the corresponding energies of the transverse acoustic phonons we were studying varied from ∼2 meV to 6.5 meV. This range of energies spans the one-triplet bandwidth between 2.8 and 3.2 meV as well as the onset of the two-triplet continuum, above ∼4.7 meV. At low temperatures, below ∼10 K, the magnetic excitation spectrum is gapped below the one-triplet excitation, ∼2.8 meV, and also between the one and two triplet bands, from ∼3.2 meV to ∼4.7 meV. If appreciable interaction or hybridization occurred between the low-lying acoustic phonons and the low-lying spin excitations, the gapped structure of the magnetic excitation spectrum below 10 K would be expected to manifest itself in the phonons. One natural manifestation of such an interaction could be the removal of a decay channel for the phonons, were their lifetimes influenced by the decay of the phonon into a combination of lower energy phonon plus magnetic excitation. Indeed, as described below, this is consistent with what we observe.

The constant-**Q** measurements at representative temperatures of 3 K, 15 K, and 30 K are shown in the left-hand panels of Fig. 4. These data sets have been fitted to an appropriate resolution convolution of a Bose temperature factor multiplied by a damped harmonic oscillator form for $\chi''(\mathbf{Q},\hbar\omega)$:

$$S(\mathbf{Q},\omega,T) = \chi(\mathbf{Q},T)\frac{1}{1-\exp\left(-\frac{\hbar\omega}{kT}\right)} \times\left[\frac{4\omega\Gamma_{\mathbf{Q},T}/\pi}{\left(\omega^2-\Omega_{\mathbf{Q},T}^2\right)^2+4\omega^2\Gamma_{\mathbf{Q},T}^2}\right], \quad (2)$$

where $\chi(\mathbf{Q}, T)$ is the momentum-dependent susceptibility, while the second term takes into account detailed balance. The renormalized damped harmonic oscillator frequency $\Omega_{\mathbf{Q}}$ has contributions from the oscillation frequency $\omega_{\mathbf{Q},T}$ and the damping coefficient $\Gamma_{\mathbf{Q},T}$, and is given by $\Omega_{\mathbf{Q},T}^2 = \omega_{\mathbf{Q},T}^2 + \Gamma_{\mathbf{Q},T}^2$.

The right-hand panel of Fig. 4 shows the same data, but with an energy-independent background removed and the result has been multiplied through by the Bose factor, thereby isolating $\chi''(\mathbf{Q},\hbar\omega)$ as a function of $\hbar\omega$. This clearly shows that $\chi''(\mathbf{Q}, \omega)$ is temperature independent between 3 K and 30 K for low-energy transverse acoustic phonons below ∼4.5 meV, but not for the higher energy transverse acoustic phonons, which become qualitatively sharper in energy at the lowest temperatures, within the singlet ground state. The solid lines in all the Fig. 4 panels are the results of fitting a resolution convolution of Eq. (2) to the data, and clearly this provides a good description to the data at all **Q**'s and temperatures measured.

The damping coefficient $\Gamma_{\mathbf{Q},T}$, which is inversely proportional to the lifetime of the appropriate transverse acoustic phonon at wave vector **Q** and temperature $T$, was extracted from this fitting and it is plotted as a function of temperature for different phonon energies in Fig. 5(a) and as a function

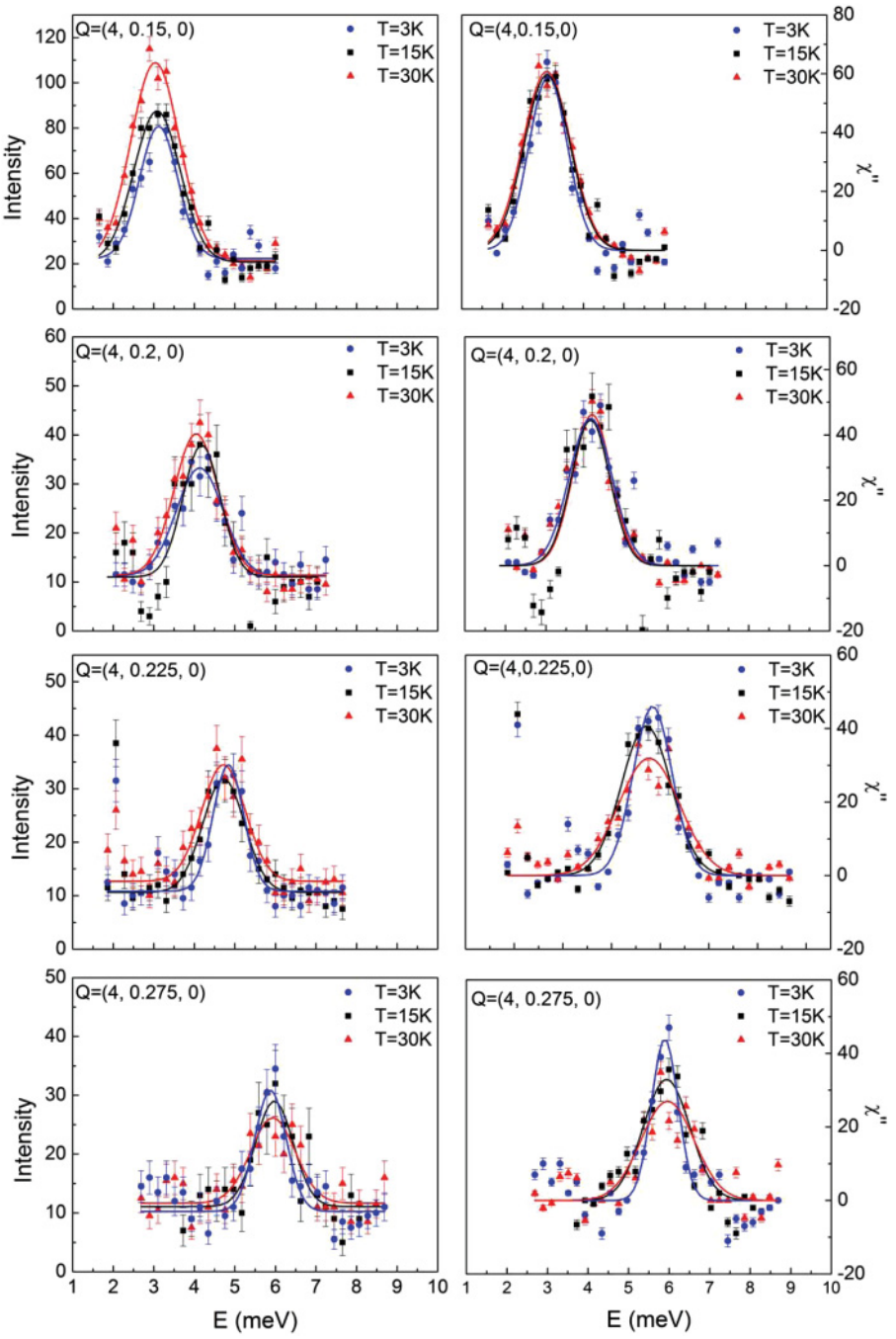


FIG. 4. (Color online) Constant-**Q** neutron scans (left-hand panels) are shown for **Q** = (4, 0.15, 0), (4, 0.2, 0), (4, 0.225, 0), and (4, 0.275, 0), from top to bottom. The corresponding energies of these transverse acoustic phonons range from ∼3 to 6 meV, spanning the region from near the 1-triplet energy to within the 2-triplet continuum. The right-hand panels show the resulting $\chi''$, which is related to the measured magnetic scattering, $S(\mathbf{Q}, \omega)$ through Eq. (2). The three data sets shown in each panel are at $T = 3$ K (well within the singlet ground state), 15 K, and 30 K (well within the paramagnetic state). The solid lines shown are resolution-convoluted fits of the data to appropriate damped harmonic oscillator line shapes [Eq. (2)].

of energy for different temperatures in Fig. 5(b). The trend in Fig. 5 is clear: Transverse acoustic phonons propagating along $(H, 0, 0)$ have long lifetimes for energies above the approximate onset of the two-triplet continuum and for temperatures less than 10 K, the onset of the singlet ground state. These higher energy transverse acoustic phonons have lifetimes which can be made longer by the gapping of the magnetic excitation spectrum below ∼4.7 meV. Lower energy phonons cannot decay into a combination of excitations at least one of which is a spin excitation whose energy is higher than that of the original phonon. Removal of this density of one or two two-triplet states would be expected to have a smaller effect on the lifetimes of such low-energy phonons.

While it is interesting that the lifetimes of the relatively high energy transverse acoustic phonons increase strongly on $SrCu_2(BO_3)_2$ entering its singlet ground state, it is also interesting that the low-energy ones do not. Rather, and somewhat unexpectedly, the low-energy transverse acoustic phonons possess finite and largely temperature-independent lifetimes for all temperatures below ∼100 K. It appears that some interaction with other degrees of freedom maintain a finite lifetime even in the absence of thermal fluctuations at low

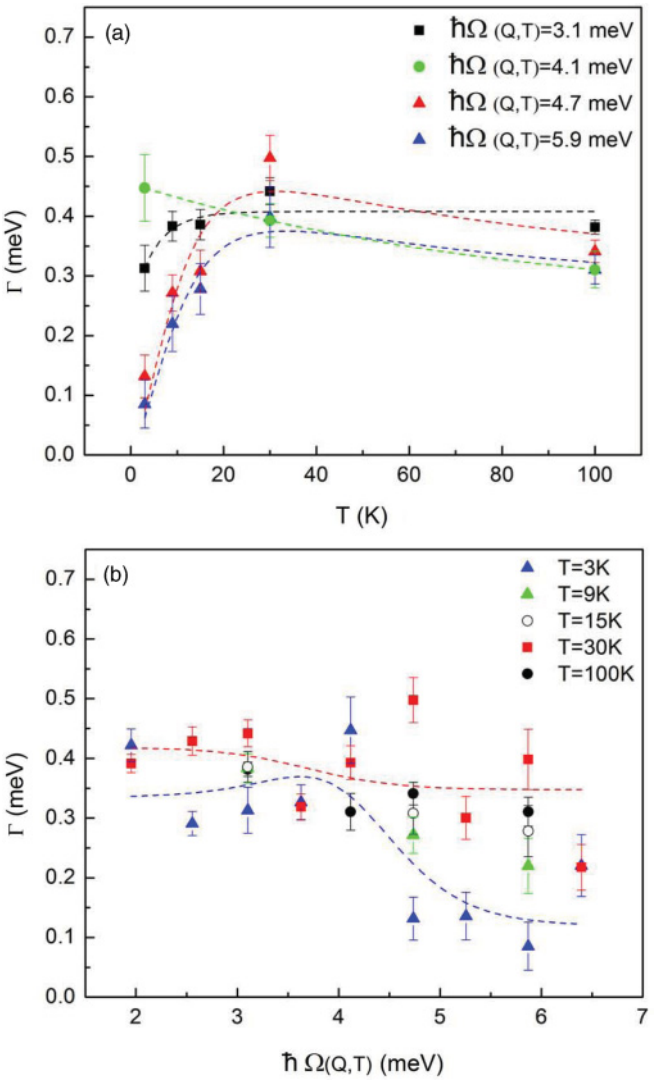


FIG. 5. (Color online) The inverse lifetimes (Γ) of the transverse acoustic phonons as function of temperature for different energies (a) and as a function of energy for different temperatures (b) are shown. These values were extracted from fits of the data in Fig. 4 to a resolution convolution of Eq. (2), in which the transverse acoustic line shape is treated as a damped harmonic oscillator. It is clear that only the higher energy, low-temperature transverse acoustic phonons show resolution-limited behavior, and hence long lifetimes.

temperatures for transverse acoustic phonons with energies below the onset of the two-triplet continuum (∼4.7 meV).

## V. CONCLUSION

In conclusion, we have investigated the role of the lattice in the formation of the singlet ground state of the quasi-two-dimensional Shastry-Sutherland quantum magnet $SrCu_2(BO_3)_2$. We performed a new neutron powder diffraction study which failed to detect evidence for a structural phase transition on entering the low-temperature singlet ground state below ∼10 K in our sample, consistent with earlier work.[24] Such a possibility had been raised by earlier heat capacity measurements. We carried out extensive inelastic neutron scattering studies of the transverse and longitudinal acoustic phonons propagating in the ($H$, 0, 0) direction within the Shastry-Sutherland plane. A survey of these acoustic phonons shows the zone boundary acoustic phonons at ∼16 meV. Higher resolution triple-axis measurements investigated the temperature dependence of the low-lying transverse acoustic phonons. Interestingly, transverse acoustic phonons with energies greater than or equal to the onset of the two-triplet continuum at ∼4.7 meV display significantly enhanced lifetimes on entering the low-temperature singlet ground state. This is attributed to removal of a decay mechanism for these phonons in which the phonons decay into a combination of excitations involving low-energy spin excitations. The spin excitation spectrum is gapped within the singlet ground state such that little or no density of spin excitation states exists below ∼2.8 meV or between ∼3.2 and 4.7 meV. We also observe an unexpected temperature independence to the transverse acoustic phonons with energies less than ∼4.7 meV, suggesting that they maintain interactions with some degrees of freedom well into the singlet ground state. Taken together these measurements demonstrate an intriguing coupling between spin and lattice degrees of freedom, but not one which obviously manifests itself in a structural phase transition on entering the singlet ground state, as occurs in spin-Peierls-like materials. We hope this work motivates further theoretical and experimental studies of such subtle effects on the intriguing quantum ground state in $SrCu_2(BO_3)_2$.

## ACKNOWLEDGMENTS

We wish to acknowledge expert technical support from CNBC, Chalk River, as well as from the ISIS User Group. This work benefited from discussions with T. Ziman. This work was supported by NSERC of Canada.

*Current address: The Advanced Photon Source, Argonne National Laboratory, Argonne, Illinois 60439, USA and The James Franck Institute and Department of Physics, The University of Chicago, Chicago, Illinois 60637, USA.

†Current address: Department of Physics, Munich Technical University, James Franck Strasse 1, Garching D-85748, Germany.

[1]See, for example, E. Dagotto and T. M. Rice, Science **271**, 618 (1996); in *Dynamical Properties of Unconventional Magnetic Systems*, edited by A. T. Skjeltorp and D. Sherrington, NATO ASI Series, Series E, Applied Sciences, Vol. 349 (Kluwer Academic Publishers, Boston, 1998).

[2]B. S. Shastry and B. Sutherland, Physica B + C **108**, 1069 (1981).

[3]S. Miyahara and K. Ueda, Phys. Rev. Lett. **82**, 3701 (1999).

[4]H. Kageyama, K. Yoshimura, R. Stern, N. V. Mushnikov, K. Onizuka, M. Kato, K. Kosuge, C. P. Slichter, T. Goto, and Y. Ueda, Phys. Rev. Lett. **82**, 3168 (1999).

[5]R. W. Smith and D. A. Keszler, J. Solid State Chem. **93**, 430 (1991).
[6]H. Kageyama, M. Nishi, N. Aso, K. Onizuka, T. Yosihama, K. Nukui, K. Kodama, K. Kakurai, and Y. Ueda, Phys. Rev. Lett. **84**, 5876 (2000).
[7]O. Cépas, K. Kakurai, L. P. Regnault, T. Ziman, J. P. Boucher, N. Aso, M. Nishi, H. Kageyama, and Y. Ueda, Phys. Rev. Lett. **87**, 167205 (2001).
[8]K. Kakurai, in *Quantum Properties of Low Dimensional Antiferromagnets*, edited by A. Ajiro and J. P. Boucher (Kyushu University Press, Fukuoka, 2002).
[9]B. D. Gaulin, S. H. Lee, S. Haravifard, J. P. Castellan, A. J. Berlinsky, H. A. Dabkowska, Y. Qiu, and J. R. D. Copley, Phys. Rev. Lett. **93**, 267202 (2004).
[10]A. Zorko, D. Arčon, H. van Tol, L. C. Brunel, and H. Kageyama, Phys. Rev. B **69**, 174420 (2004).
[11]H. Nojiri, H. Kageyama, Y. Ueda, and M. Motokawa, J. Phys. Soc. Jpn. **72**, 3243 (2003).
[12]S. El Shawish, J. Bonča, and I. Sega, Phys. Rev. B **72**, 184409 (2005).
[13]M. Miyahara and K. Ueda, J. Phys.: Condens. Matter **15**, R327 (2003).
[14]K. Kodama, M. Takigawa, M. Horvatić, C. Berthier, H. Kageyama, Y. Ueda, S. Miyahara, F. Becca, and F. Mila, Science **298**, 395 (2002).
[15]K. Onizuka, H. Kageyama, Y. Narumi, K. Kindo, Y. Ueda, and T. Goto, J. Phys. Soc. Jpn. **69**, 1016 (2000).
[16]G. A. Jorge, R. Stern, M. Jaime, N. Harrison, J. Bonca, S. E. Shawish, C. D. Batista, H. A. Dabkowska, and B. D. Gaulin, Phys. Rev. B **71**, 092403 (2005).
[17]S. E. Sebastian, N. Harrison, P. Sengupta, C. D. Batista, S. Francoual, E. Palm, T. Murphy, N. Marcano, H. A. Dabkowska, and B. D. Gaulin, Proc. Natl. Acad. Sci. USA **105**, 20157 (2008).
[18]H. Kageyama, K. Onizuka, T. Yamauchi, Y. Ueda, S. Hane, H. Mitamura, T. Goto, K. Yoshimura, and K. Kosuge, J. Phys. Soc. Jpn. **68**, 1821 (1999).
[19]K. Sparta, G. J. Redhammer, P. Roussel, G. Heeger, G. Roth, P. Lemmens, A. Ionescu, M. Grove, G. Güntherodt, F. Hüning, H. Lueken, H. Kageyama, K. Onizuka, and Y. Ueda, Eur. Phys. J. **19**, 507 (2001).
[20]M. Hase, I. Terasaki, and K. Uchinokura, Phys. Rev. Lett. **70**, 3651 (1993).
[21]M. D. Lumsden and B. D. Gaulin, Phys. Rev. B **59**, 9372 (1999).
[22]M. Isobe and Y. Ueda, J. Phys. Soc. Jpn. **65**, 1178 (1996).
[23]C. C. Homes, S. V. Dordevic, A. Gozar, G. Blumberg, T. Room, D. Huvonen, U. Nagel, A. D. LaForge, D. N. Basov, and H. Kageyama, Phys. Rev. B **79**, 125101 (2009).
[24]C. Vecchini, O. Adamopoulos, L. C. Chapon, A. Lappas, H. Kageyama, Y. Ueda, and A. Zorko, J. Solid State Chem. **182**, 3275 (2009).